nature physics

SUPPLEMENTARY INFORMATION

DOI: 10.1038/NPHYS1821

SUPPLEMENTARY INFORMATION FOR "EXPERIMENTAL DEMONSTRATION OF INFORMATION-TO-ENERGY CONVERSION AND VALIDATION OF THE GENERALIZED JARZYNSKI EQUALITY"

Shoichi Toyabe,[1] Takahiro Sagawa,[2] Masahito Ueda,[2,3] Eiro Muneyuki,[1] and Masaki Sano[2]

[1]*Department of Physics, Faculty of Science and Engineering, Chuo University, Kasuga, Tokyo 112-8551, Japan*
[2]*Department of Physics, Graduate School of Science, University of Tokyo, Hongo, Tokyo 113-0033, Japan*
[3]*ERATO Macroscopic Quantum Control Project, JST, Yayoi, Tokyo 113-8656, Japan*

A. SCHEMATIC OF EXPERIMENT AND THE CONSISTENCY WITH THE SECOND LAW OF THERMODYNAMICS.

We demonstrated that free energy is obtained by a feedback control using the information about the system; information is converted to free energy, as the first realization of Szilard-type Maxwell's demon[1].

Since the obtained free energy or work is compensated for by the demon's energy cost to manipulate information, it does not violate the second law of thermodynamics when the total system including both the particle and demon is considered. The demon consists of macroscopic devices in practice such as computers in our system; the microscopic device gains energy at the expense of the energy consumption of a macroscopic device (Fig. S1). In other words, by using information as the energy-transferring "medium", this information-energy conversion can be utilized to transport energy to nanomachines even if it is not possible to drive them directly.

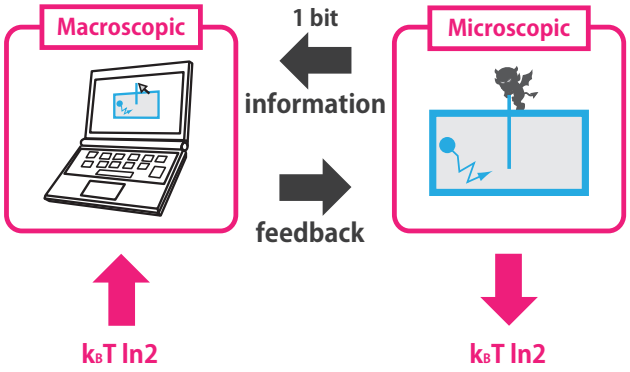

Figure S 1: Schematic of the information-energy conversion with a macroscopic demon and a microscopic system (Szilard engine[1] as an example). The Szilard-engine can achieve the 100% conversion rate from information to energy; 1 bit ($\ln 2$ nat in the natural logarithm) of information is converted to free energy or work of $k_{\mathrm{B}}T\ln 2$ in the microscopic system at the expense of an energy consumption of $k_{\mathrm{B}}T\ln 2$ in the macroscopic demon.

B. PREPARATION OF CHAMBER.

Brownian particles in a buffer solution were prepared for the experiment by the following procedure. The cover slip (Matsunami, Japan) that served as the ceiling of the observation chamber was washed three times with distilled water. The bottom glass coated with chromium electrodes (Matsunami, Japan) was soaked in 10 N KOH over night and then washed with distilled water. The top and bottom glasses were separated by a plastic film with a thickness of about 12 μm (Saran wrap, Asahi Kasei, Japan) and silicone grease. 6 μl of A buffer (50 mM MOPS-K, 50 mM KCl, 2 mM $MgCl_2$, 2 mg/ml heat-shocked Bovine serum albumin (Sigma-Aldrich, USA), pH6.9) was applied to the chamber to suppress the binding of particles to the glass surface. Then, 10 μl of streptavidin-coated polystyrene beads with a diameter of 287 nm (Seradyn, USA) in A buffer was applied to the chamber. Some particles bound to the top glass surface. About 50 μl of B buffer (5 mM MOPS-K, 1 mM $MgCl_2$, 1 mM KP_i, pH6.9) was applied to wash out unbound particles in the chamber. All the experiments were performed in B buffer at a room temperature.

DOI: 10.1038/NPHYS1821

C. MICROSCOPY AND IMAGE ANALYSIS.

The incidentally-dimeric particle pinned at the top glass surface was observed on a phase-contrast microscope (BX-51WI, Olympus, Japan) equipped with a high speed camera (IPX-210L, Imperx, USA) at a period of 1.1 ms with an exposure time of 0.3 ms. Real-time feedback system was constructed on the PXI (PCI eXtensions for Instrumentation) system implementing a computing module (PXI-8108, National Instruments, USA), a video capturing board (PXI-1428, National Instruments), and a digital-to-analog conversion board for the control of the electric potential across the electrodes patterned on the bottom glass plate (PXI-6221, National Instruments). The minimum delay in this feedback control is thus 1.1 ms which is much shorter than the time for the particle to perform rotational diffusion up to 90 degrees. The angle of the dimeric probe particle was estimated using an algorithm based on the principal component analysis.

D. ROTATIONAL BROWNIAN MOTION

To confirm that particles exhibit a free Brownian motion in the absence of imposed potential, rotational trajectories of particles were observed in the absence of electric field at 7,000 Hz using a high-speed camera (A504k, Basler, Germany). Figure S2 shows the rotational trajectories, the mean square displacements, and the power spectrum density of the rotational velocity of four typical particles.

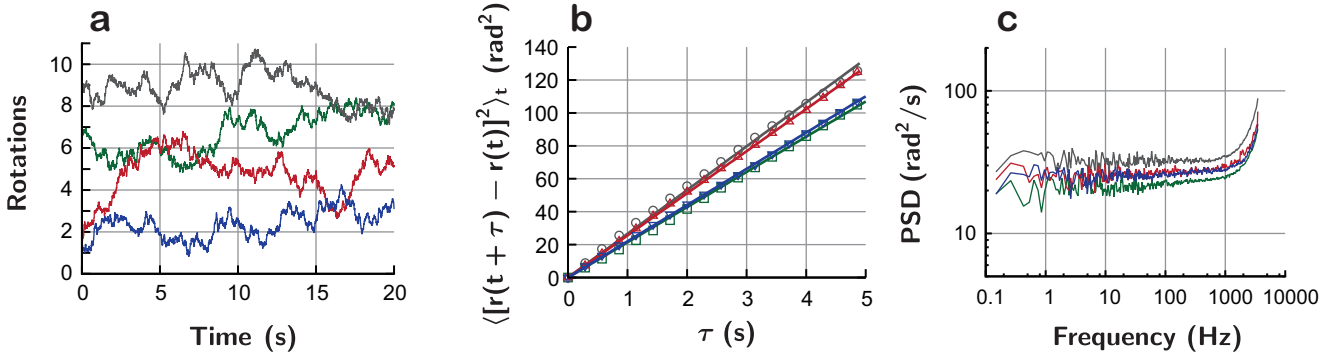

Figure S2: Confirmation that the particles can be treated as a free Brownian particle in the absence of imposed potential. Data of four typical particles are shown. Different color corresponds to different particle. The number of observed frames is typically 4×10^6 for each particle. **a**, Rotational trajectories. **b**, Mean square displacements of the rotations. Solid lines are linear fitting curves. **c**, Power spectrum density of the rotational velocity.

The mean square displacement depended linearly on time (Fig. S2b). Also, the power spectrum density of the rotational velocity was flat except the high-frequency region, where aliasing effects due the discrete samplings distort the spectrum (Fig. S2c). These results show that the particles can be treated as a free Brownian particles.

E. ELLIPTICALLY-ROTATING ELECTRIC FIELD.

To provide a periodic potential and adverse torque to the Brownian particle, we utilized the induced polarization effect of the dielectric material subjected to an AC external electric field[2–4]. Four chromium electrodes on the bottom glass surface were connected to four power amplifiers (HSA4101, NF, Japan) that amplify AC (Alternative Current) voltages generated by function generators (WF1974, NF, Japan). We applied 1-MHz AC voltages with some phase shifts on the electrodes (Fig. S3). Let the phases on the electrodes to be 0, δ, 180, and $180+\delta$ degrees. Three different types of potentials are imposed on the particle according to the value of δ (Fig. S4).

- If $\delta = \pm 90$ degrees, a rotating electric field is applied at the center of the electrodes (Fig. S4a), where a dipole moment rotating at the same rate with some time delay appears on dielectric particles. The length of the time

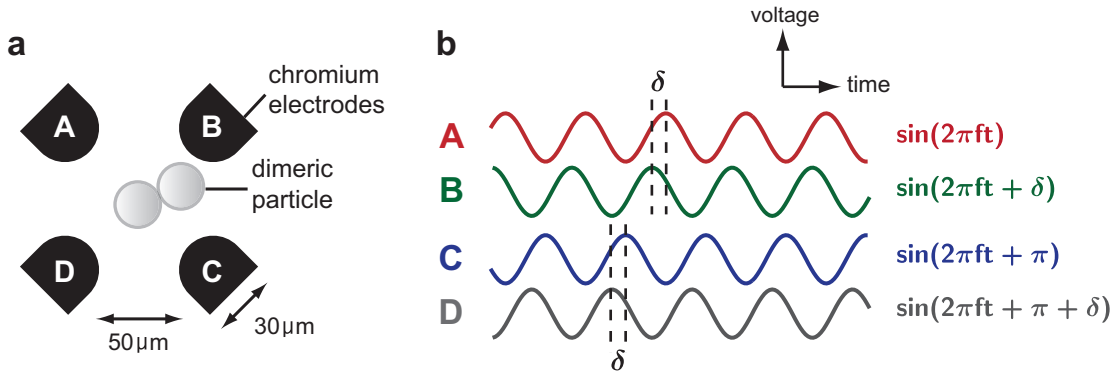

Figure S3: (a) Quadrant electrodes. Not to scale. (b) Sinusoidal voltages applied on the electrodes.

delay is determined by the complex dielectric constants of the particle and the solution. Due to the time delay, the particle experiences a torque from the electric field [2–4]. The torque is constant; it does not depend on the particle's motions but depends only on the time delay. Its magnitude is proportional to the particles's volume and the square of the amplitude of the applied AC voltages. Also, it nonlinearly depends on the frequency of the applied AC voltages. According to the sign of δ, the direction of the torque is changed.

- If $\delta = 0$ or 180 degrees, the electric field does not rotate but oscillates along an axis (Fig. S4b). In this case, because of a dielectrophoretic effect, the particle's axis goes to align in the direction of the electric field. Thus, the particle feels a periodic potential with a period of 180 degrees along the direction of rotation. By switching δ, we can change the direction of the electric field. For $\delta = 0$, $\phi_{\rm A} = \phi_{\rm B} = -\phi_{\rm C} = -\phi_{\rm D}$; the electric field directs longitudinally (we denote the phases of A, B, C, and D as $\phi_{\rm A}$, $\phi_{\rm B}$, $\phi_{\rm C}$, and $\phi_{\rm D}$, respectively). For $\delta = 180$, $\phi_{\rm A} = -\phi_{\rm B} = \phi_{\rm C} = -\phi_{\rm D}$; the electric field directs laterally. The oscillating direction of the electric field corresponds to the angle of the potential's local minima.

- Otherwise, an elliptically rotating electric field is applied (Fig. S4c); it corresponds to the superposition of the above two cases ($\delta = 0$ and 90 degrees). In such case, the particle feels a tilted periodic potential. The gradient of the potential depends on the value of δ. According to the sign of δ, the direction of the torque is changed.

We set δ to be about 5 degrees (δ was tuned for each particle) to apply the elliptically rotating electric field. For feedback control, the potential was switched by modulating the phases of applied voltages from 0, δ, 180, and 180+δ degrees to 0, 180-δ, 180, and -δ degrees, respectively for four electrodes.

F. ESTIMATION OF POTENTIAL ENERGY.

The potential profiles were estimated by a method similar to Ref. [5] (Fig. S5a). We switched two potentials with opposite phases periodically with a period of 220 ms to sample data around not only the local minima but also the peaks. We divided the whole video frames to two sets according to the potential at each frame. For each set of frames, we performed the following procedures to estimate the potential profile. 360 degrees are divided to equally-spaced bins with a bin width of 3 degrees. We counted the number of video frames $m_{\rm i}$ where the particle is in the ith bin. We also counted the number of transitions $n_{\rm i\to j}$, or the number of two-successive-frame where the particle in the ith bin moves to the jth bin at the next frame. The transition probabilities $w_{\rm i\to j} \equiv n_{\rm i\to j}/m_{\rm i}$ satisfy the detailed balance condition:

$$\frac{w_{\rm i\to j}}{w_{\rm j\to i}} = e^{-\Delta U_{\rm i\to j}/k_{\rm B}T}, \tag{S1}$$

DOI: 10.1038/NPHYS1821

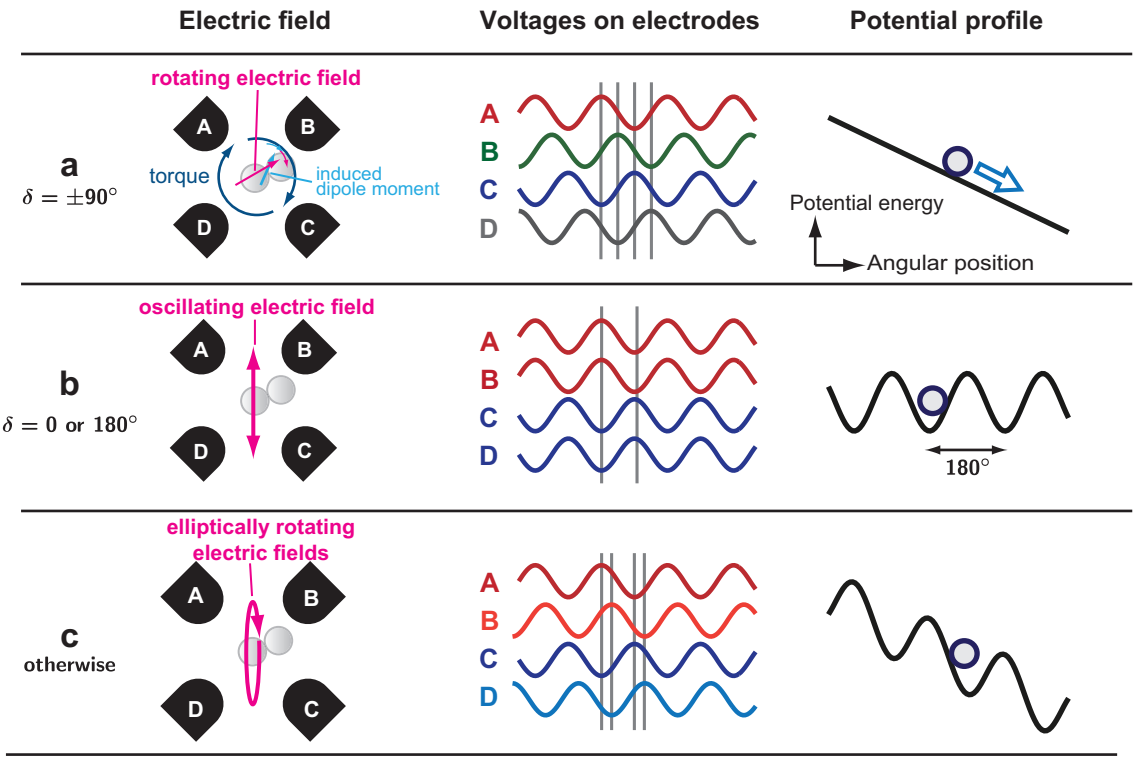

Figure S 4: Three different types of the potential imposed on the particle according to the phase shift δ. (a) Rotating electric field. (b) Oscillating electric field. (c) Elliptically rotating electric field.

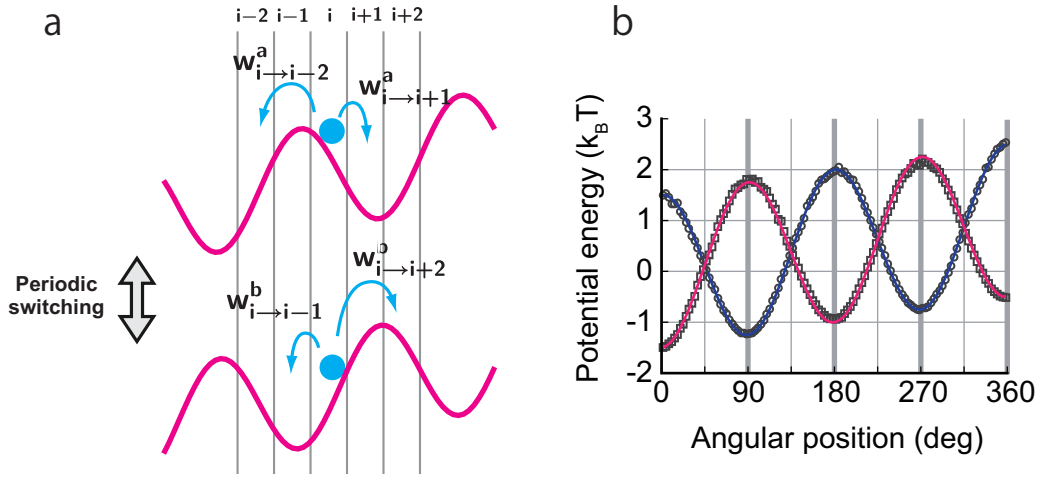

Figure S 5: (a) Potential estimation. (b) Estimation of the potential energy for a simulated trajectory. Solid lines indicate the theoretical curves. Markers correspond to estimated values (bin width = 3 degrees). The slope is 1 $k_BT/360°$, the activation energy (peak-to-peak amplitude) 3 k_BT, the rotational friction coefficient 0.3 pN·nm·s/rad^2, the frame rate 1000 Hz, and temperature 300 K. Number of frames is 1,000,000. The potentials were switched every 200 frames.

where $\Delta U_{i\to j} \equiv U_j - U_i$ is the difference of the potential energies between ith and jth bins. We searched the set $\{U_i^*\}$ which minimizes a score function as follows:

$$\varepsilon^2(\{U_i\}) \equiv \sum_{i<j} \sqrt{n_{i\to j} n_{j\to i}} \left[\Delta U_{i\to j} - \Delta U'_{i\to j}\right]^2,$$

where $\Delta U'_{i\to j} \equiv k_B T \left[\ln w_{j\to i} - \ln w_{i\to j}\right]$, using the Powell's method [6].

The validity of this method was verified for numerically-simulated trajectories based on a Langevin dynamics. Figure S5b shows that this algorithm estimates the potential energy for the trajectory generated by a Langevin simulation to a good extent.

A typical number of video frames used for the potential estimation was about 1,000,000.

G. STATE AND FREE ENERGY.

Figure S6 is the schematic to illustrate the definition of the state and how to calculate the free energy.

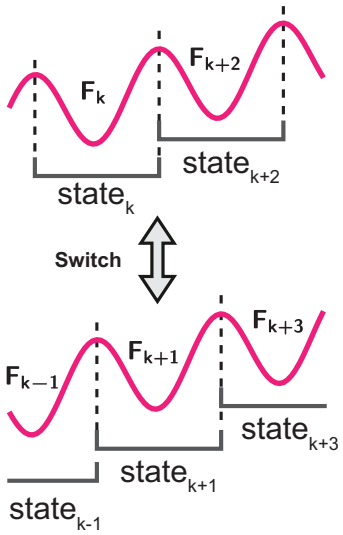

Figure S 6: Definitions of the states and free energies. The well separated by peaks is regarded as a state. A free energy is assigned to each state.

H. SCHEMATIC OF ENERGETICS.

Schematic to illustrate the energetics in a cycle with a switching is shown in Fig. S7.

I. FEEDBACK EFFICACY.

Figure S8 is the schematic to illustrate the feedback efficacy.

J. EFFICIENCY.

Figure S9 shows (a) the probability that the particle is observed in the region S, (b) the (average) Shannon information content, and (c) the efficiency to convert information to energy.

---

[1] L. Szilard, Z. Physik **53**, 840 (1929).
[2] T. Watanabe-Nakayama, S. Toyabe, S. Kudo, S. Sugiyama, M. Yoshida, and E. Muneyuki, Biochem. Biophys. Res. Comm. **366**, 951 (2008).
[3] M. Washizu, Y. Kurahashi, H. Iochi, O. Kurosawa, S. i. Aizawa, S. Kudo, Y. Magariyama, and H. Hotani, IEEE Trans. Industry Appl. **29**, 286 (1993).

DOI: 10.1038/NPHYS1821

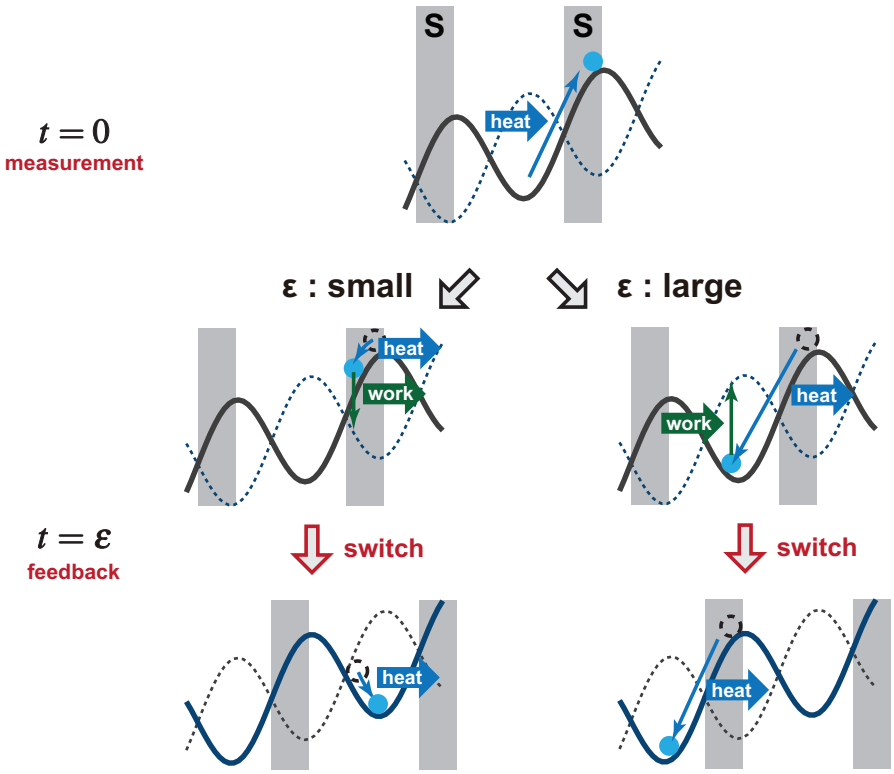

Figure S 7: Schematic to illustrate the energetics in a cycle with a switching. For small ε, switchings occur mostly when the particle is in the region S. In this case, the particle absorbs heat from an isothermal environment to reach the region S before measurements at $t = 0$, performs extractable work to the electric field at the switching, and finally jumps to the rightward well after the switching. On the other hand, for large ε, most of the energy at $t = 0$ dissipates to the heat bath before switching. Then, the switching performs external work on the particle with lifting up the potential, which then dissipates as it falls down in the well.

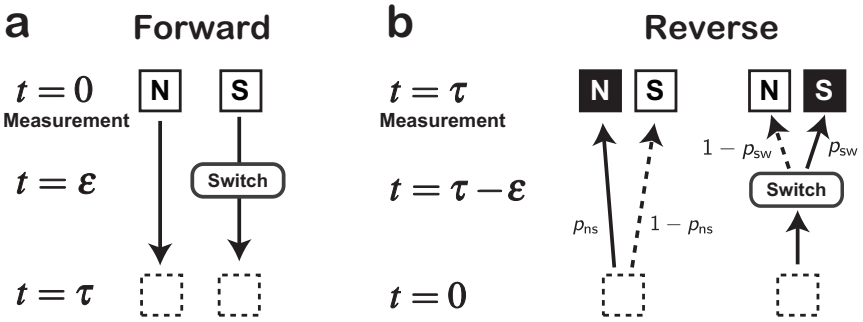

Figure S 8: Forward and reversed cycle. (A) Forward feedback cycle. "S" and "N" indicate that the particle is observed in the region S or not, respectively. (B) Reversed cycle. Feedback control is not performed.

[4] S. Toyabe, T. Okamoto, T. Watanabe-Nakayama, H. Taketani, S. Kudo, and E. Muneyuki, Phys. Rev. lett. **104**, 198103 (2010).
[5] J. R. Errigton, J. Chem. Phys. **120**, 3130 (2004).
[6] W. H. Press, S. A. Teukolsky, W. T. Vetterling, and B. P. Flannery, *Nuperical Recipes Third Edition* (Cambridge University Press, 2007).

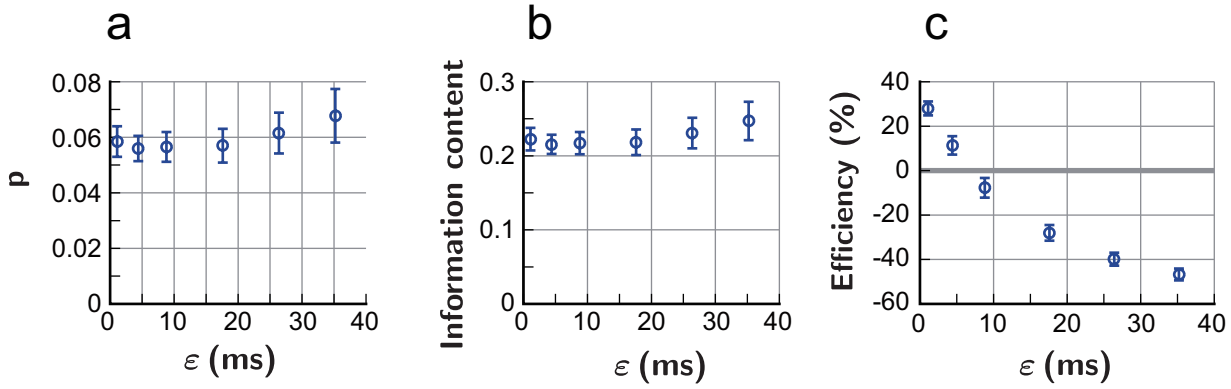

Figure S 9: Efficiency of information-energy conversion. (a) The probability p that the particle is observed in the region S. (b) Shannon information content $I \equiv -p \ln p - (1-p)\ln(1-p)$. (c) Efficiency of the information-energy conversion calculated as $\langle \Delta F - W \rangle / k_{\mathrm{B}} T I$. Error bars indicate standard deviations among particles.